



Obrabotka metallov - Metal Working and Material Science

Journal homepage: http://journals.nstu.ru/obrabotka_metallov



Normal force influence on smoothing and hardening of steel 03Cr16Ni15Mo3Ti1 surface layer during dry diamond burnishing with spherical indenter

Viktor Kuznetsov^{1, 2, 3, a, *}, Aleksey Makarov^{1, b}, Andrey Skorobogatov^{3, c}, Polina Skorynina^{4, d},
Sergey Luchko^{1, e}, Vitalij Sirosh^{1, f}, Nikolay Chekan^{5, g}

¹ M.N. Miheev Institute of Metal Physics, Ural Branch of the Russian Academy of Sciences, 18 S. Kovalevskoy str., Ekaterinburg, 620108, Russian Federation

² Ural Federal University named after the first President of Russia B.N. Yeltsin, 19 Mira str., Ekaterinburg, 620002, Russian Federation

³ Federal State Budgetary Institution "National Ilizarov Medical Research Centre for Traumatology and Orthopaedics" Ministry Healthcare, Russian Federation, 6 M. Ulyanova st., Kurgan, 640014, Russian Federation

⁴ Institute of Engineering Science Ural Branch, Russian Academy of Sciences, 34 Komsomolskaya st., Ekaterinburg, 620049, Russian Federation

⁵ Physical-Technical Institute of National Academy of Sciences of Belarus, 10 Akademika Kuprevicha st., Minsk, 220141, Belarus

^a <https://orcid.org/0000-0001-8949-6345>, wpkuzn@mail.ru, ^b <https://orcid.org/0000-0002-2228-0643>, avm@imp.uran.ru,

^c <https://orcid.org/0000-0001-7447-1962>, ufo2log@gmail.com, ^d <https://orcid.org/0000-0002-8904-7600>, polina.skorynina@mail.ru,

^e <https://orcid.org/0000-0002-2368-0913>, serojaluchko@gmail.com, ^f <https://orcid.org/0000-0002-8180-9543>, sirosh.imp@yandex.ru,

^g <https://orcid.org/0000-0002-3339-9922>, chekan@phti.by

ARTICLE INFO

Article history:

Received: 15 December 2021

Revised: 03 January 2022

Accepted: 15 January 2022

Available online: 15 March 2022

Keywords:

Austenitic steel
 Finish turning
 Diamond burnishing
 Burnishing force
 Roughness
 Microhardness

Funding

The research was supported by the Russian Foundation for Basic Research and the Belarusian Republican Foundation for Fundamental Research (Project No. 20-58-00057) and carried out within the state assignments of the Institute of Metal Physics, RAS (Ural Branch) on the topic No. AAAA-A18-118020190116-6 and the Institute of Engineering Science, RAS (Ural Branch) on the topic No. AAAA-A18-118020790148-1.

Acknowledgements

Research were partially conducted at core facility "Structure, mechanical and physical properties of materials"

For citation: Kuznetsov V.P., Makarov A.V., Skorobogatov A.S., Skorynina P.A., Luchko S.N., Sirosh V.A., Chekan N.M. Normal force influence on smoothing and hardening of steel 03Cr16Ni15Mo3Ti1 surface layer during dry diamond burnishing with spherical indenter. *Obrabotka metallov (tehnologiya, oborudovanie, instrumenty) = Metal Working and Material Science*, 2022, vol. 24, no. 1, pp. 6–22. DOI: 10.17212/1994-6309-2022-24.1-6-22. (In Russian).

* Corresponding author

Kuznetsov Viktor P., D.Sc. (Engineering), Professor
 Ural Federal University
 named after the first President of Russia B.N. Yeltsin, 19 Mira st.,
 620002, Ekaterinburg, Russia
 Tel.: 8 (982) 422-17-77, e-mail: wpkuzn@mail.ru

ABSTRACT

Introduction. Sliding burnishing minimizes roughness and hardens of the steel surface. Quality of the formed surface and strength characteristics of the surface layer are determined by the burnishing speed, force and feed. Due to the danger of the surface micro-destruction during burnishing, the problem of selecting the favorable value of the normal force at a given feed arises. **The current investigation aims** to study the effect of normal force during dry diamond burnishing with a spherical indenter on smoothing the surface microprofile and strain hardening of the 03Cr16Ni15Mo3Ti1 austenitic steel surface layer. **Research methods.** Profilometry, scanning electron microscopy (SEM), microdurometry are used. **Results and discussion.** As the result of dry burnishing of deformation-stable austenitic steel 03Cr16Ni15Mo3Ti1 with a spherical indenter with a 2 mm radius made of natural diamond at a sliding speed of 10 m/min and feed rate of 0.025 mm/rev, it is found that in the investigated variation range of the burnishing normal force (100...200 N) the value of the smoothing coefficient of the initial steel surface microprofile after finish turning is 79...90 %, the greatest smoothing with a decrease in the average roughness parameter R_a from 1.0 to 0.1 μm is achieved at a force of 150 N; during diamond burnishing the initial (after finish turning) surface is hardened by 15...43 % (up to 382...444 HV), as the burnishing force raises from 100 to 175 N, a non-monotonic increase of the average microhardness from 409 to 444 HV 0.05 takes place; burnishing with a load of 175 N forms a gradient-hardened layer with a thickness of 300...350 μm with the appearance of individual microfractures in the form of beadings and micro-cracks on the surface, the maximum hardening is caused by the formation of a highly dispersed surface layer of 30...40 μm thick with a structure of highly dispersed austenite and the corresponding activation of grain-boundary and dislocation strengthening mechanisms. The results can be used when selecting the diamond burnishing parameters of parts made of corrosion-resistant austenitic steels according to the criteria for obtaining low surface roughness without significant microfractures and effective strain hardening of the surface layer.

Introduction

Austenitic stainless chromium-nickel steels, due to high level of corrosion resistance, plasticity, heat resistance, manufacturability and biocompatibility [1-3], are widely applied in the oil and gas, chemical, nuclear, food and medical industries.

For many critical applications, steels of $01Cr17Ni13Mo3$ type (analog *AISI 316L*) are of particular interest. These steels retain corrosion resistance under mechanical influences due to its low tendency to martensitic deformation transformation [4], and are also prospective to be used in hydrogen economy as a hydrogen embrittlement-resistant material for hydrogen transportation and storage systems [5]. Dispersion-hardening steel of $Cr16Ni15Mo3Ti1$ type is additionally alloyed with ~1 wt.% titanium, which provides radiation-stimulated release of the coherent γ' -phase (Ni_3Ti) and thereby multiplies the resistance to void (vacancy) swelling during irradiation with high-speed neutrons at temperatures of 480...500 °C [6-9]. Therefore, it is prospective as not only corrosion-resistant, but also radiation-resistant material, operable in the presence of aggressive environments.

The microhardness of non-heat-treatable *AISI 316L* steel surface can be increased by ultrasonic treatment with a carbide spherical indenter (from 177 to 290 HV) [10] and balls in vacuum – by *SMAT*: surface mechanical attrition treatment (from 1.65 to 2.90 GPa) [11], by sandblasting (from 1.8 to 3.6 GPa) [12]. However, the surface layers formed during impact hardening treatments are characterized by high roughness $Ra = 1.0...2.5 \mu m$ [11, 12]. Significantly more effective hardening of $03Cr16Ni14Mo3Ti1$ steel surface (from 270 to 580...720 HV 0.025) can be achieved by friction treatment with a sliding indenter made of synthetic diamond in an argon medium [13]. Such processing of austenitic chromium-nickel steels can also provide high quality of the formed surface with low roughness [14, 15].

Sliding burnishing of steels minimizes roughness and strengthens the surface layer. The surface quality and strength characteristics of the surface layer formed during burnishing are determined by the speed, feed and force of burnishing, the size of the contact area and multiplicity of loading [16-23]. The paper [16] shows the possibility of controlling surface layer smoothing and strengthening based on the evaluation of the integral parameter of the multiplicity of material loading during the burnishing process. When considering diamond burnishing of stainless *17-4 PH* steel, the feed is determined by the most significant parameter affecting surface roughness and hardness [17]. Under conditions of dry ball burnishing, the best roughness smoothing of the turned surface of *41Cr4* steel was provided by a small feed of 0.05 mm/rev, in contrast to 0.075 mm/rev and 0.1 mm/rev [18].

On the contrary, in [19], when studying the ball burnishing of *AISI 1045* steel, it was found that the greatest influence on both the surface roughness and hardness is exerted by the burnishing force. The normal force is also a parameter determining a high level of compressive residual stresses (-1,100 MPa) being formed by ball burnishing on the *15-5PH* martensitic stainless-steel surface [20]. The depth of spherical indenter penetration (determined by normal force, microhardness and roughness of the work surface), at which complete smoothing of the initial roughness is achieved, is proposed in [21] as a criterion for ensuring minimal roughness when burnishing hardened steels and is called stable indentation. An increase in the normal force and contact spot size, as well as a decrease in the feed to increase the multiplicity of loading and hardening of the material being treated, can cause micro-destruction of the work surface. In this regard, at diamond burnishing, there is a problem of the exact assignment of the normal force at a given feed.

Maximov et al. in [22] noted that there is no data in the literature on the prospects of sliding indenter burnishing of *AISI 316Ti* ($03Cr16Ni10Mo2Ti$) austenitic steel, which is closest in chemical composition to the steel under study. However, the new results obtained in [22] do not allow establishing a connection between the normal force and surface microprofiles, both after turning and after burnishing. In addition, when choosing the burnishing force, it is important to assign it from the standpoint of material strengthening.

3D surface profilometry during the transition from turning to diamond burnishing of disks made of *AISI 304* metastable austenitic steel is considered in [23]. However, the assignment of the normal loading force of the surface layer during burnishing was not validated.

The purpose of this work is to study the effect of the normal force during dry diamond burnishing with a spherical indenter on smoothing of turned surface microprofile and on deformation hardening of the *03Cr16Ni15Mo3Ti1* austenitic steel surface layer.

Research methodology

The study of dry surface burnishing was performed on austenitic stainless steel *03Cr16Ni15Mo3Ti1* ($C - 0.03\%$; $Cr - 16.64\%$; $Ni - 14.96\%$; $Mo - 2.77\%$; $Ti - 1.25\%$; $Si - 0.53\%$; $Mn - 0.38\%$; $Cu - 0.11\%$; $P - 0.03\%$; $S - 0.02\%$; the rest – Fe). The experimental samples of the “disk” type with a diameter of 104 mm and a thickness of 19 mm were subjected to heat treatment – quenching from the temperature of 1,100 °C (exposure time of 1 hour) with cooling in water. After quenching at the *Takisawa EX-310* turning and milling center, the finish turning of the sample end surface was performed with a *WNMG080408* tool plate using a lubricating and cooling water-emulsion process medium (*LCPM*) at a cutting speed of 150 m/min, a feed of 0.08 mm/rev and a cutting depth of 0.3 mm. After turning, the average surface roughness was $Ra = 1.0\ \mu\text{m}$, and the microhardness was $311 \pm 10\ \text{HV}\ 0.05$ and $331 \pm 9\ \text{HV}\ 0.2$.

Further, after turning, concentric ring sections with a width of 5 mm were burnished on the treated sample surface (Fig. 1). Burnishing was carried out with a tool able to adjust the burnishing force and to use a spherical indenter with a radius of 2 mm made of natural diamond without using *LCPM* (in air). The burnishing force varied according to the data of Table. The range of force variation from 100 to 200 N was selected in accordance with the study of burnishing *AISI 316Ti* analog steel, which was made by *Maximov et al.* [24]. In accordance with this study, the feed value $f_b = 0.025\ \text{mm/rev}$ was taken.

The choice of the indenter sliding speed ($v_s = 10\ \text{m/min}$) is justified by the maximum permissible speed of dry burnishing the stainless high-chromium steel surface found in [25]. Exceeding the permissible sliding speed leads to a significant increase in roughness and surface layer micro-fractures occurrence.

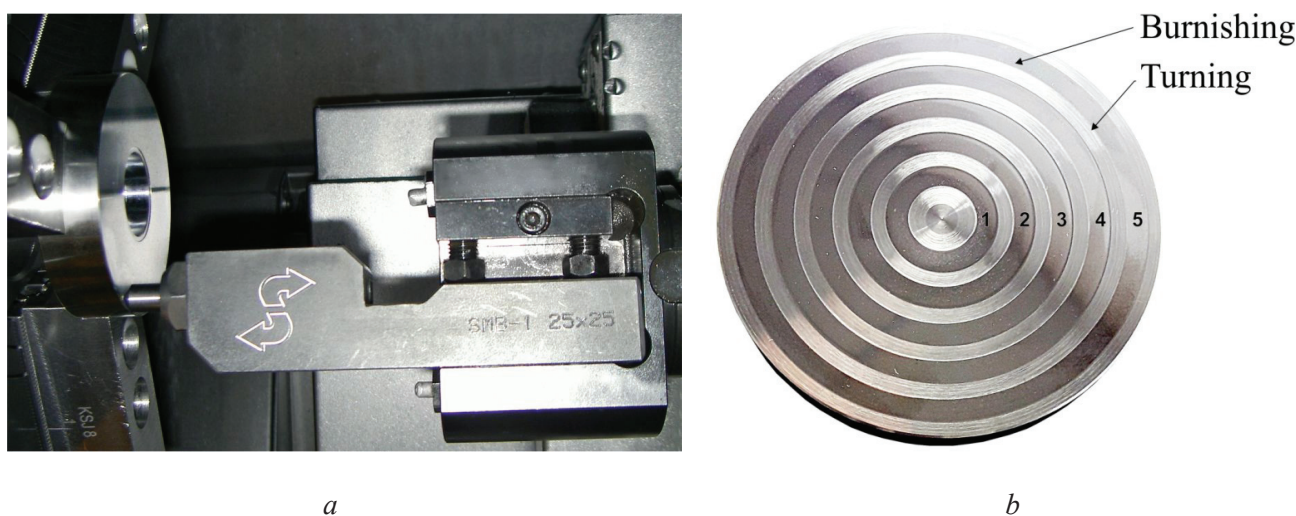


Fig. 1. Burnishing of the sample surface on the turning-milling center (a) and annular sections (b), indicated by numbers according to the given burnishing force given in Table

Parameters of dry diamond burnishing of ring sections

Mode	Burnishing force F_b , N	Sliding speed v_s m/min	Feed rate f_b , mm/rev
1	200	10	0.025
2	175		
3	150		
4	125		
5	100		

The surface roughness was studied by 3D profilometry with a *WYKO NT-1100* device. 3D profilograms were obtained and the average values of the parameter Ra (the arithmetic mean deviation of the profile) were determined according to the analysis of three surface areas with dimensions of 0.9×1.2 mm and 42.5×55.8 μm . Based on the 3D profilometry results, the surface microprofile smoothing coefficient was calculated based on the approach proposed in [26]:

$$\delta_{Ra} = \frac{Ra_t - Ra_b}{Ra_t} \cdot 100 \% \quad (1)$$

where Ra_t – is the surface roughness after previous (turning) processing; Ra_b – is the surface roughness after diamond burnishing.

The measurement of the surface microhardness was performed with the *AHOTECHEcoHARD XM1270C* microhardness tester at loads of 0.49 N (50 gf) and 1.96 N (200 gf) on the Vickers indenter. Using the results of surface micro-durometry, the hardening coefficient was calculated based on the dependence:

$$\delta_{HV} = \frac{HV_b - HV_t}{HV_t} \cdot 100 \%, \quad (2)$$

where HV_b is the microhardness after surface diamond burnishing; HV_t is the initial microhardness of the turned surface.

The change in microhardness in the surface layer depth was determined with a cross-section using a *SHIMADZU HMV-G21DT* microhardness tester under load on a Vickers indenter of 0.245 N (25 gf).

Using the *Tescan VEGA II XMU* scanning electron microscope, the samples surface and the structure of the near-surface layers in cross-sections were studied.

Results and discussion

In Fig. 2 and Fig. 3a, the results of optical 3D profilometry of the sample surface after turning and dry diamond burnishing in the zones of 0.9×1.2 mm in size are presented. It can be seen that diamond burnishing led to a significant smoothing of the initial surface roughness and a corresponding decrease in the value of the arithmetic mean deviation of the Ra profile. As the burnishing force increased from 100 to 150 N, the average value of the roughness parameter Ra decreased from 0.21 to 0.10 μm . A further increase in the burnishing force to 175 and 200 N, on the contrary, caused an increase in the average value of Ra to 0.11 and 0.17 μm , respectively (see Fig. 3a).

Calculation by formula (1) showed (Fig. 3b) that in the process of diamond burnishing of an austenitic steel disc in the range of the forces under study, the smoothing coefficient δ_{Ra} ranges from 79 to 90 % with a maximum in the case of using a load $F_b = 150$ N. Thus, according to the criterion of the profile arithmetic mean deviation, the specified most favorable normal load mode provides smoothing of the microprofile by 90 % formed by finishing turning ($Ra = 1.0$ μm), and results in nanoroughness ($Ra = 100$ nm) even on relatively extended surface areas with dimensions of 0.9×1.2 mm.

The surface microprofile analysis taken in the process of 3D profilometry at microsections with dimension 42.5×55.8 μm showed that, in contrast to the surface after turning with characteristic unidirectional large protrusions and depressions (Fig. 4a), isolated depressions are observed on the entire area of the burnished surface (Fig. 4b-d). With burnishing force of 100 N, these depressions take a shape elongated in the direction of tool movement (Fig. 4b). As burnishing force increases, the size of depressions decreases significantly, it acquires a rounded or oval shape; its distribution becomes more uniform, and the number of depressions increases (Fig. 4c, d). At the same time, the depression depth seems to decrease with an increase in burnishing force, as evidenced by a continuous decrease in the values of the roughness parameter Ra (see Fig. 4 b-d).

The presence of the revealed depressions on the burnished surfaces may be due to the insufficient amount of the burnishing force and the surface profile depressions left from the previous turning (Fig. 5a). In particular, this reason can justify the presence of elongated extended depressions on the surface burnished with a minimum investigated force of 100 N (see Fig. 4b). On the other hand, an increase in the number of

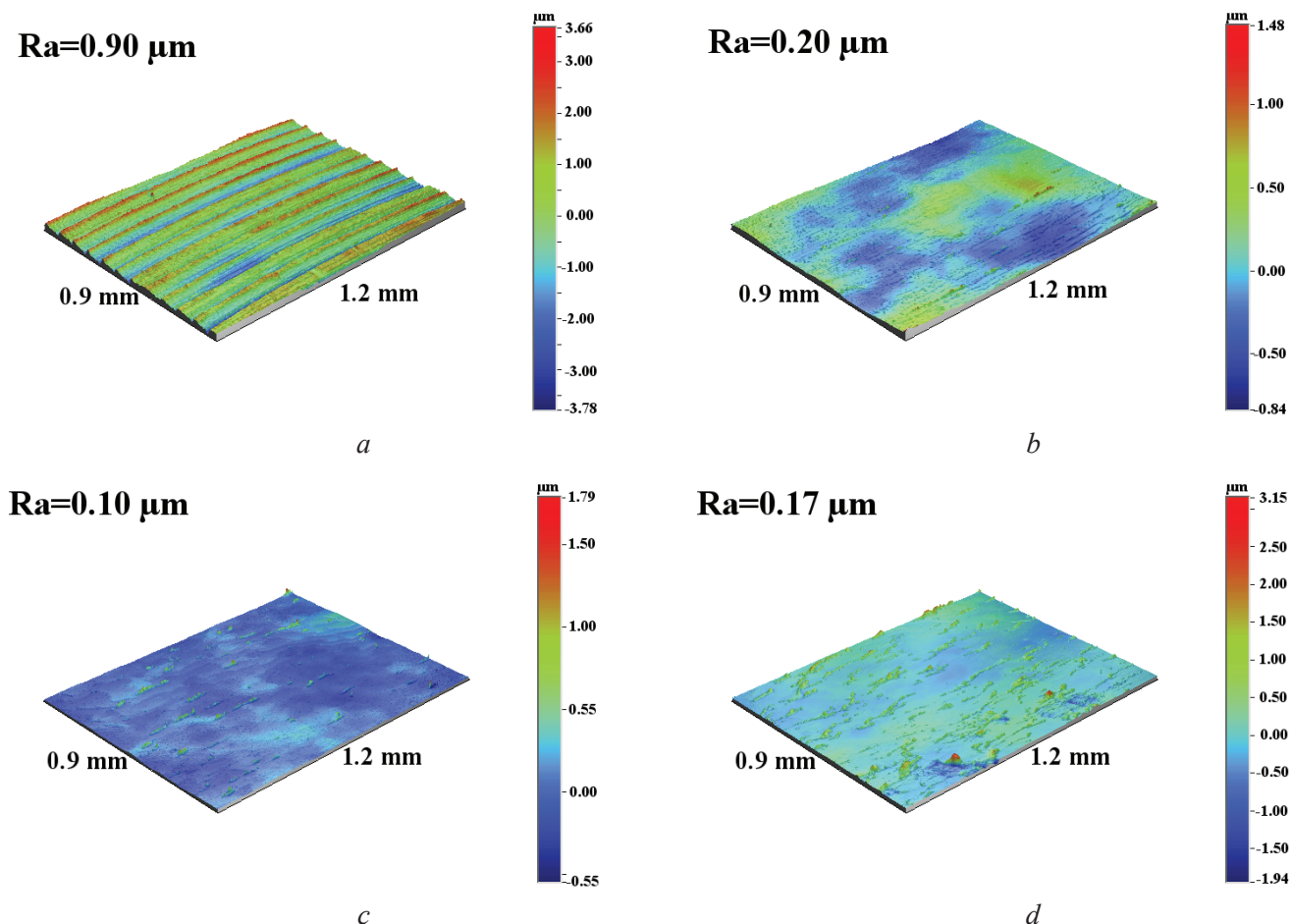


Fig. 2. Three-dimensional profilograms on a 0.9×1.2 mm area of the disk surface made of $03Cr16Ni15Mo3Ti1$ steel, after finishing turning (a) and dry diamond burnishing with different forces F_b : 100 N (b), 150 N (c) and 200 N (d)

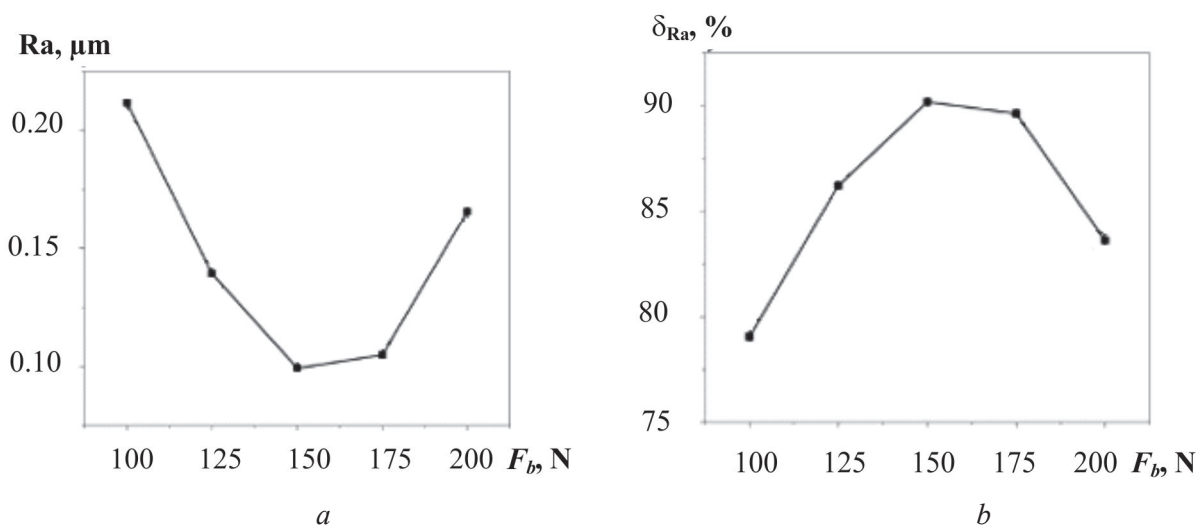


Fig. 3. Dependence of the average values of the roughness parameter R_a (a) and the smoothing coefficient δ_{Ra} (b) of the $03Cr16Ni15Mo3Ti1$ steel surface on the burnishing force F_b

depressions (indentation) during burnishing with increased loads may result from damage to the austenitic steel surface during its adhesive interaction with a diamond indenter without applying coolant lubricant.

Microdurometry of the burnished surface, performed at loads of 0.49 N and 1.96 N with the Vickers indenter, showed a significant effect of the smoothing force on the hardening of the surface layer

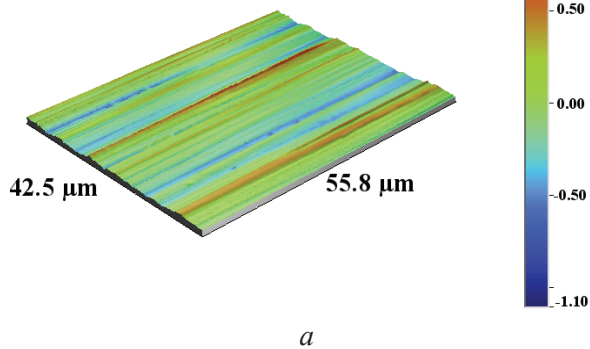
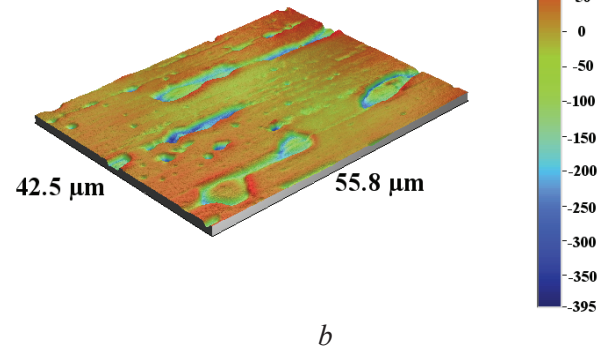
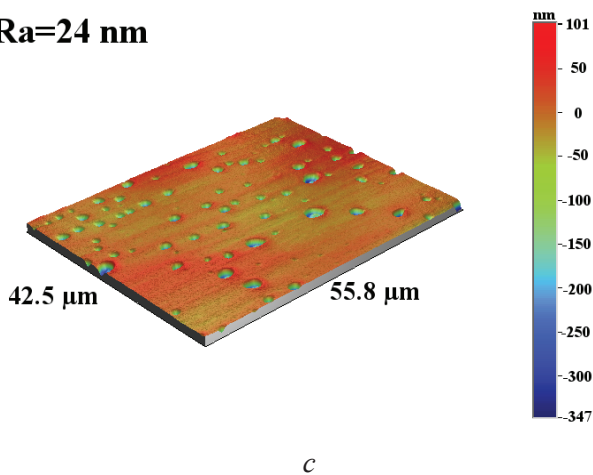
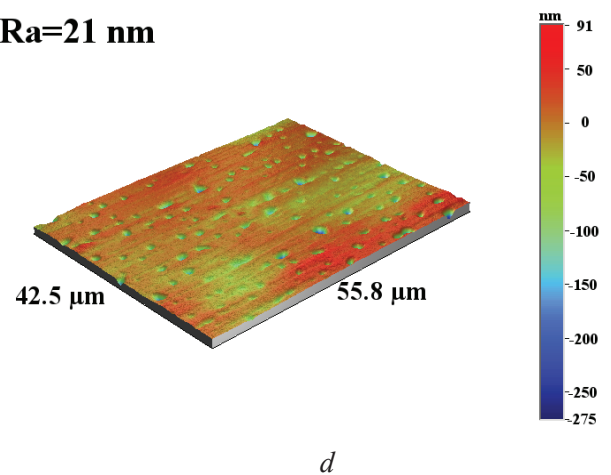
Ra=179 nm

Ra=41 nm

Ra=24 nm

Ra=21 nm


Fig. 4. Three-dimensional profilograms taken in a $42.5 \times 55.8 \mu\text{m}$ area of the disk surface made of $03\text{Cr}16\text{Ni}15\text{Mo}3\text{Ti}1$ steel, after processing by finish turning (*a*) and dry diamond burnishing with different forces F_b : 100 N (*b*), 150 N (*c*), 200 N (*d*)

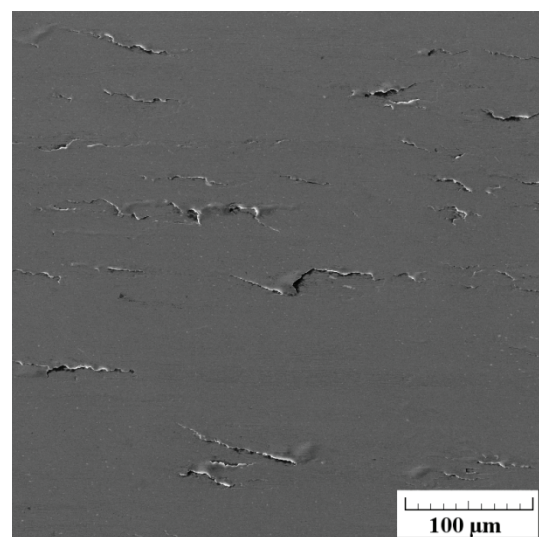
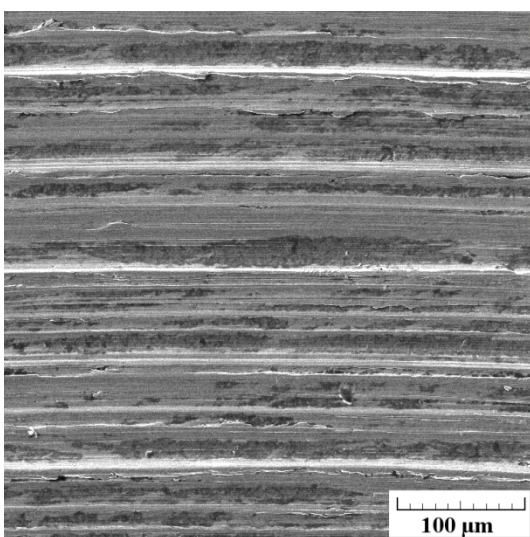


Fig. 5. SEM images of the surface of a disk made of steel $03\text{Cr}16\text{Ni}15\text{Mo}3\text{Ti}1$ after processing by finishing turning (*a*) and dry diamond burnishing with a force $F_b = 175 \text{ N}$ (*b*)

material (Fig. 6). When measuring with a load of 0.49 N, as the burnishing force increases from 100 to 175 N, a non-monotonic increase in microhardness occurs from 409 ± 17 HV 0.05 to 444 ± 7 HV 0.05 (see Fig. 6a). The established maximum level of steel surface microhardness after burnishing with a load of 175 N is observed despite individual micro-destructions in the form of buildups and microcracks as a result of metal reformation under burnishing effect (Fig. 5b).

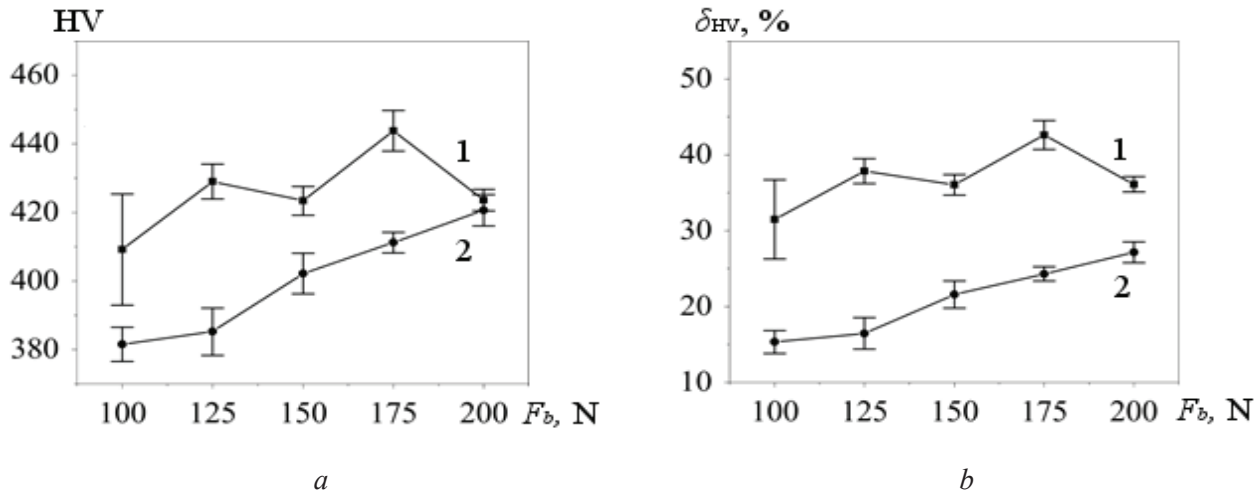


Fig. 6. Dependences of microhardness HV (a) and the hardening coefficient δ_{HV} (b) of the 03Cr16Ni15Mo-3Ti1 steel surface on the burnishing force F_b ; microhardness measurements at loads on the Vickers indenter 0.49 N (curves 1) and 1.96 N (curves 2)

With a further increase in the burnishing force to 200 N, a decrease in the microhardness of the deformed surface to 422 ± 3 HV 0.05 is observed (Fig. 6a). This can be explained by an occurrence, at the maximum burnishing force, of an over-peening effect, which leads to accumulation of surface damage and local destruction of the thin steel surface layer. This statement is supported by occurrence of noticeable irregularities on the 3D profilogram of the smoothed surface (see Fig. 2d) and a corresponding abrupt increase in roughness after a burnishing force increase from 175 to 200 N (see Fig. 3a).

From the data of Fig. 6a it also follows that at measurements using a higher load on the Vickers indenter (of 1.96 N) with increasing the burnishing force, the microhardness of the work surface increases monotonically from 382 ± 4 HV 0.2 after burnishing with a force of 100 N and achieves maximum 421 ± 4 HV 0.2 after burnishing with a force of 200 N. Consequently, the microhardness reduction HV 0.05, associated with the re-peening when increasing burnishing force from 175 to 200 N, affects only a very thin near-surface layer.

Figure 6b shows the effect of the burnishing force on the hardening coefficient δ_{HV} calculated by formula (2) when burnishing with respect to the microhardness of the initial (after turning) surface of the steel under study. A lower level of initial microhardness (310 ± 10 HV 0.05), found when measuring a thinner layer with a load of 0.49 N than when using a load of 1.96 N (330 ± 9 HV 0.2), indicates damage accumulation directly on the steel surface during the finish turning process, causing some material softening. According to Fig. 6b diamond burnishing provided 31...43 % hardening in a thin near-surface layer with an extremum at a burnishing force of 175 N and 15...27 % hardening in a thicker surface layer with a maximum microhardness at a burnishing force of 200 N.

Fig. 7 shows microhardness distribution in depth of the gradient-hardened steel surface layer after burnishing at a load of 175 N, which provided a maximum microhardness of 444 ± 7 HV 0.05 of the burnished surface. While moving away from the burnishing surface, the microhardness measured at a load of 0.245 N decreases from 400...420 HV 0.025 to 220...250 HV 0.025 at a depth of 300...350 μm .

The study of cross-sections with a scanning electron microscope showed that after finishing turning, the large austenitic grain structure is preserved in the sample surface layer (Fig. 8a). Since the technological turning (lathe machining) is designed for sizing cut, accelerated removal of the material cuttings does not create favorable conditions to accumulate large degrees of plastic deformation and structure dispersion accompanying this process in the workpiece surface layer.

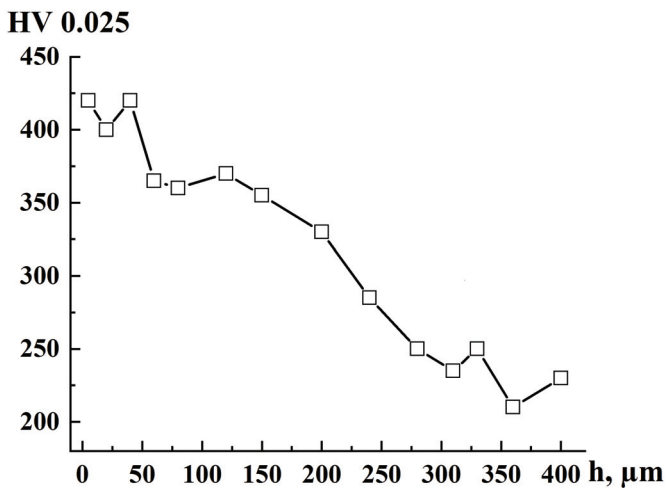


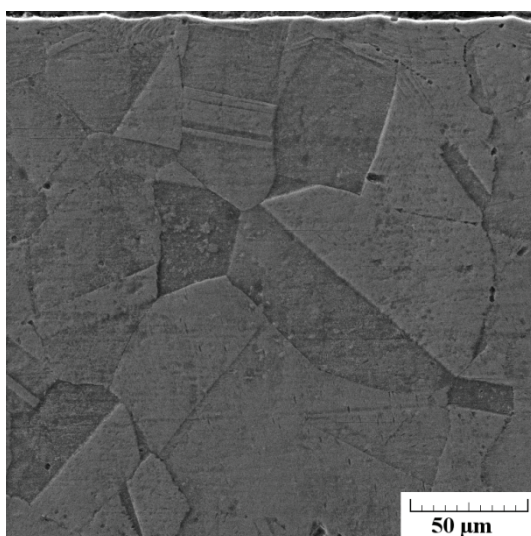
Fig. 7. Change in the microhardness HV 0.025 in depth of the 03Cr16Ni15Mo3Ti1 steel surface layer (h is the distance from the surface) after dry diamond burnishing with a force $F_b = 175$ N

occur as well due to the fact that during the passage of the sliding indenter and its individual microasperity, the metal moves from the zone of compressive stresses, in which deformation occurs in the shear conditions under pressure, into the zone of external tensile stresses [31, 32]. According to [33], the pores in metals under intense plastic deformation are formed precisely in the tension zones, while highly dispersed structures occur only in the zones of shear (compression). Tensile stresses also cause microcracking on the steel surface during burnishing (see Fig. 5b).

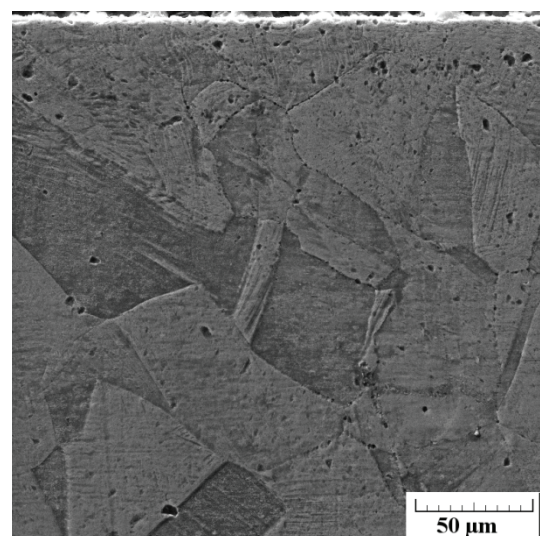
It is important to note that the highly dispersed layer dotted in Fig. 8b is characterized by a maximum microhardness level of 400...420 HV 0.025 (see Fig. 7). Thus, during microdurometric measurements with loads of 0.245, 0.49 and 1.96 N on the Vickers indenter after dry burnishing with a natural diamond indenter with a force of 175 N, a microhardness level of 400...444 HV was registered on the surface of 03Cr16Ni15Mo3Ti1 austenitic steel and in a surface layer with a thickness of 40 μm. (see Fig. 6a; 7).

In contrast to turning, dry diamond burnishing with a force of 175 N formed a pronounced surface layer with a thickness of 30...40 μm with a strongly deformed highly dispersed structure (the layer is marked with a dotted line in Fig. 8b). It can be seen that the deformation led not only to significant austenitic structure dispersion, but also to occurrence of discontinuities in the form of micropores of various sizes – from fractions of a micrometer up to 5 μm (Fig. 8b). Similar micropores were formed in a thin surface layer of AISI 321 metastable austenitic steel as a result of friction treatment with a synthetic diamond indenter in an argon medium [27, 28].

It is known that micropores of deformation origin (submicropores) in plastic metallic materials are formed in the process of submicrocrack blunting that appear in deformable metal when moving dislocations are blocked by barriers such as inclusions, grain boundaries, sliding lines, etc. [29, 30]. Micropores



a



b

Fig. 8. The structure of the 03Cr16Ni15Mo3Ti1 steel surface layer after finish turning (a) and dry diamond burnishing with the force of $F_b = 175$ N (b); cross-section, scanning electron microscopy, the dotted line indicates the layer boundary with dispersed structure



A similar level of deformation hardening (up to 4.1...4.4 GPa) was observed as a result of intensive plastic chromium-nickel austenitic steel deformation by ultrasonic impact treatment with strikers [34], ultrasonic peening in vacuum [35] and equal-channel angular pressing (extrusion) [36]. When processing a workpiece made of *AISI 304* metastable austenitic steel by finishing turning and diamond burnishing with lubricating fluid on a turning and milling center, hardening on the surface and surface layer with a thickness of 75 μm to 380...450 HV 0.025 was achieved [23].

Nanostructuring surface machining *SMAT* of *316L (02Cr17Ni12Mo2Mn2)* austenitic steel, similar in composition to *03Cr16Ni15Mo3Ti1* steel studied in this work, led to surface hardening up to 4.5 GPa [37, 38] and surface layer nanostructuring with a thickness of 40 μm with formation of 15 % nanocrystalline strain-induced martensite.

In our earlier study [13], on the surface of *03Cr16Ni14Mo3Ti1* austenitic steel under the conditions of friction treatment with a sliding indenter made of synthetic diamond in a nonoxidizing argon medium, an increase in microhardness up to 720 HV 0.025 was observed with a total depth of a gradient-hardened layer of 300 μm . A high coefficient of friction ($f = 0.47$) in the process of friction treatment with a synthetic diamond indenter [13] contributed to more intensive steel hardening than in this work, while when burnishing with a natural diamond indenter, even without lubricating fluid, the coefficient of friction does not exceed 0.1 [39].

In contrast to the works [37, 38], the study [13] observed an almost complete absence of deformation $\gamma \rightarrow \alpha$ transformation: in a surface layer $\sim 7 \mu\text{m}$ thick, no more than 1.5% (vol.) of strain-induced α' -martensite was formed during friction treatment of *03Cr16Ni14Mo3Ti1* steel. The noted result is due to the increased content of nickel (a strong austenite stabilizer) in *03Cr16Ni14Mo3Ti1* steel compared with its amount in *316L (02Cr17Ni12Mo2Mn2)* steel [37, 38]. At the same time, in [13], as a result of friction treatment, nano- and submicrocrystalline austenitic structures were formed on the surface of *03Cr16Ni14Mo3Ti1* steel, the occurrence of which was preceded by generation of dislocation cell and band structures. The formation in stable-to-deformation and metastable austenitic steels under frictional impact of highly disordered crystals of nano- and submicrometer dimensions [13-15, 40] occurs at the final stage of structure transformation due to cell turns and its decrement as a result of the development of a rotational deformation mechanism due to friction [41].

Thus, the established increase in microhardness of stable-to-deformation *03Cr16Ni15Mo3Ti1* austenitic steel to 400...444 HV as a result of dry burnishing with an indenter made of natural diamond can be explained by formation of highly dispersed austenite in the surface layer and by corresponding activation of grain boundary and dislocation mechanisms of hardening.

Conclusions

As a result of the experimental study of the normal force magnitude effect during dry burnishing by a spherical indenter with a radius of 2 mm made of natural diamond at a sliding speed of 10 m/min and a feed value of 0.025 mm/rev on the surface roughness formation and surface layer hardening of stable-to-deformation *03Cr16Ni15Mo3Ti1* austenitic steel, it is established:

1) in the studied variation range of the normal burnishing force of 100...200 N, the smoothing coefficient of the steel surface initial microprofile after finish turning is 79...90 %, the greatest smoothing with a decrease in the average roughness parameter R_a from 1.0 to 0.1 μm is achieved at a force of 150 N;

2) with diamond burnishing, the initial (after turning) surface is strengthened by 15...43 % (up to 382...444 HV), as the burnishing force increases from 100 to 175 N, a non-monotonic increase in the average microhardness occurs from 409 to 444 HV 0.05

3) burnishing with a load of 175 N forms a gradient-hardened layer with a thickness of 300...350 μm with generated individual micro-fractures on the surface in the form of buildups and microcracks, the maximum hardening of the steel surface is due to formation of a highly dispersed surface layer with a thickness of 30...40 μm with a structure of highly dispersed austenite and corresponding activation of grain boundary and dislocation mechanisms of hardening.



The results obtained can be used in the scientifically justified selection of technological parameters for diamond burnishing of workpieces made of corrosion-resistant austenitic steels according to the criteria for obtaining a high-quality surface (with low roughness in the absence of significant micro-fractures) and effective deformation hardening of the surface layer.

References

1. Lo K.H., Shek C.H., Lai J.K.L. Recent developments in stainless steels. *Materials Science and Engineering: R: Reports*, 2009, vol. 65, iss. 4–6, pp. 39–104. DOI: 10.1016/j.mser.2009.03.001.
2. Borgioli F. From austenitic stainless steel to expanded austenite-S phase: formation, characteristics and properties of an elusive metastable phase. *Metals*, 2020, vol. 10, iss. 2, art. 187. DOI: 10.3390/met10020187.
3. Solomon N., Solomon I. Effect of deformation-induced phase transformation on AISI 316 stainless steel corrosion resistance. *Engineering Failure Analysis*, 2017, vol. 79, pp. 865–875. DOI: 10.1016/j.engfailanal.2017.05.031.
4. Astafurova E.G., Melnikov E.V., Astafurov S.V., Ratochka I.V., Mishin I.P., Maier G.G., Moskvina V.A., Zakharov G.N., Smirnov A.I., Bataev V.A. Hydrogen embrittlement effects on austenitic stainless steels with ultrafine-grained structure of different morphology. *Physical Mesomechanics*, 2018, vol. 22, iss. 4, pp. 313–326. DOI: 10.1134/S1029959919040076.
5. Melnikov E.V., Maier G.G., Moskvina V.A., Astafurova E.G. Vliyanie nasyshcheniya vodorodom na strukturu i mekhanicheskie svoystva austenitnoi stali 01Kh17N13M3 [Influence of hydrogen saturation on the structure and mechanical properties of Fe-17Cr-13Ni-3Mo-0.01C austenitic steel during rolling at different temperatures]. *Obrabotka metallov (tekhnologiya, oborudovanie, instrumenty) = Metal Working and Material Science*, 2021, vol. 23, iss. 2, pp. 81–97. DOI: 10.17212/1994-6309-2021-23.2-81-97.
6. Sagaradze V.V., Pavlov V.A., Alyabiev V.M., Goshchitskiy B.N., Kozlov A.V., Lapin S.S., Loguntsev Ye.N., Nalesnik V.M., Khakhalkin N.V., Shalayev V.I., Gaydukov M.G., Sergeev G.A. The influence of intermetallic ageing during irradiation by fast neutrons on void formation in austenitic stainless steels. *Physics of Metals and Metallography*, 1988, vol. 65, iss. 5, pp. 128–135.
7. Sagaradze V.V., Nalesnik V.M., Shejnkman A.G., Bibilashvili Yu.K., Aljab'ev V.M., Barsanov V.I., Kozlov A.V., Lapin S.S., Pavlov V.A., Saraev O.M., Uvarov A.I., Shalaev V.I. *Stal'* [Steel]. Patent RF, no. 1807735, 1995.
8. Sagaradze V.V., Nalesnik V.M., Lapin S.S., Aliabev V.M. Precipitation hardening and radiation damageability of austenitic stainless steels. *Journal of Nuclear Materials*, 1993, vol. 202, iss. 1–2, pp. 137–144. DOI: 10.1016/0022-3115(93)90036-X.
9. Sagaradze V.V., Lapin S.S. Unconventional approaches to the suppression of irradiation-induced swelling of stainless steels. *The Physics of Metals and Metallography*, 1997, vol. 83, iss. 4, pp. 417–427.
10. Wang C., Han J., Zhao J., Song Y., Man J., Zhu H., Sun J., Fang L. Enhanced wear resistance of 316 L stainless steel with a nanostructured surface layer prepared by ultrasonic surface rolling. *Coatings*, 2019, vol. 9, iss. 4, art. 276. DOI: 10.3390/coatings9040276.
11. Arifvianto B., Suyitno, Mahardika M. Effects of surface mechanical attrition treatment (SMAT) on a rough surface of AISI 316L stainless steel. *Applied Surface Science*, 2012, vol. 258, iss. 10, pp. 4538–4543. DOI: 10.1016/j.apsusc.2012.01.021.
12. Suyitno, Arifvianto B., Widodo T.D., Mahardika M., Dewo P., Salim U.A. Effect of cold working and sandblasting on the microhardness, tensile strength and corrosion resistance of AISI 316L stainless steel. *International Journal of Minerals, Metallurgy and Materials*, 2012, vol. 19, iss. 12, pp. 1093–1099. DOI: 10.1007/s12613-012-0676-1.
13. Makarov A.V., Skorynina P.A., Volkova E.G., Osintseva A.L. Effect of friction treatment on the structure, micromechanical and tribological properties of austenitic steel 03Kh16N14M3T. *Metal Science and Heat Treatment*, 2020, vol. 61, iss. 11–12, pp. 764–768. DOI: 10.1007/s11041-020-00497-1.
14. Makarov A.V., Skorynina P.A., Osintseva A.L., Yurovskikh A.S., Savrai R.A. Povyshenie tribologicheskikh svoystv austenitnoi stali 12Kh18N10T nanostrukturiruyushchei friktsionnoi obrabotkoi [Improving the tribological properties of austenitic 12Kh18N10T steel by nanostructuring frictional treatment]. *Obrabotka metallov (tekhnologiya, oborudovanie, instrumenty) = Metal Working and Material Science*, 2015, no. 4 (69), pp. 80–92. DOI: 10.17212/1994-6309-2015-4-80-92.
15. Makarov A.V., Skorynina P.A., Yurovskikh A.S., Osintseva A.L. Effect of the conditions of the nanostructuring frictional treatment process on the structural and phase states and the strengthening of metastable austenitic steel. *Physics of Metals and Metallography*, 2017, vol. 118, iss. 12, pp. 1225–1235. DOI: 10.1134/S0031918X17120092.



16. Kuznetsov V.P., Smolin I.Yu., Dmitriev A.I., Tarasov S.Yu., Gorgots V.G. Toward control of subsurface strain accumulation in nanostructuring burnishing on thermostrengthened steel. *Surface and Coatings Technology*, 2016, vol. 285, pp. 171–178. DOI: 10.1016/j.surfcoat.2015.11.045.
17. Sachin B., Narendranath S., Chakradhar D. Analysis of surface hardness and surface roughness in diamond burnishing of 17-4 PH stainless steel. *IOP Conference Series: Materials Science and Engineering*, 2019, vol. 577, art. 012075. DOI: 10.1088/1757-899X/577/1/012075.
18. Grzesik W., Zak K. Characterization of surface integrity produced by sequential dry hard turning and ball burnishing operations. *Journal of Manufacturing Science and Engineering*, 2014, vol. 136, iss. 3, art. 031017. DOI: 10.1115/1.4026936.
19. Saldaña-Robles Al., Plascencia-Mora H., Aguilera-Gómez E., Saldaña-Robles Ad., Marquez-Herrera A., Diosdado-De la Peña J.A. Influence of ball-burnishing on roughness, hardness and corrosion resistance of AISI 1045 steel. *Surface and Coatings Technology*, 2008, vol. 339, pp. 191–198. DOI: 10.1016/j.surfcoat.2018.02.013.
20. Chomienne V., Valiorgue F., Rech J., Verdu C. Influence of ball burnishing on residual stress profile of a 15-5PH stainless steel. *CIRP Journal of Manufacturing Science and Technology*, 2016, vol. 13, pp. 90–96. DOI: 10.1016/j.cirpj.2015.12.003.
21. Shiou F.-J., Hsu C.-C. Surface finishing of hardened and tempered stainless tool steel using sequential ball grinding, ball burnishing and ball polishing processes on a machining centre. *Journal of Materials Processing Technology*, 2008, vol. 205, iss. 1–3, pp. 249–258. DOI: 10.1016/j.jmatprotec.2007.11.244.
22. Maximov J.T., Duncheva G.V., Anchev A.P., Ganey N., Amudjev I.M., Dunchev V.P. Effect of slide burnishing method on the surface integrity of AISI 316Ti chromium–nickel steel. *Journal of the Brazilian Society of Mechanical Sciences and Engineering*, 2018, vol. 40, iss. 4, art. 194. DOI: 10.1007/s40430-018-1135-3.
23. Kuznetsov V.P., Makarov A.V., Osintseva A.L., Yurovskikh A.S., Savrai R.A., Rogovaya S.A., Kiryakov A.E. Uprochnenie i povyshenie kachestva poverkhnosti detalei iz austenitnoi nerzhavayushchei stali almaznym vyglazhivaniem na tokarno-frezernom tsentre [The increase of strength and surface quality of austenitic stainless steel parts by diamond burnishing on the turning-milling center]. *Uprochnyayushchie tekhnologii i pokrytiya = Strengthening Technologies and Coatings*, 2011, no. 11, pp. 16–26.
24. Maximov J.T., Anchev A.P., Duncheva G.V., Ganey N., Selimov K.F. Influence of the process parameters on the surface roughness, micro-hardness, and residual stresses in slide burnishing of high-strength aluminum alloys. *Journal of the Brazilian Society of Mechanical Sciences and Engineering*, 2017, vol. 39, pp. 3067–3078. DOI: 10.1007/s40430-016-0647-y.
25. Kuznetsov V.P., Tarasov S.Yu., Dmitriev A.I. Nanostructuring burnishing and subsurface shear instability. *Journal of Materials Processing Technology*, 2015, vol. 217, pp. 327–335. DOI: 10.1016/j.jmatprotec.2014.11.023.
26. Sin'kevich Yu.V., Sheleg V.K., Yankovskii I.N., Belyaev G.Ya. *Elektroimpul'snoe polirovanie na osnove zheleza, khroma i nikelya* [Electric pulse polishing based on iron, chromium and nickel]. Minsk, BNTU Publ., 2014. 325 p. ISBN 978-985-550-516-2.
27. Savrai R.A., Osintseva A.L. Effect of hardened surface layer obtained by frictional treatment on the contact endurance of the AISI 321 stainless steel under contact gigacycle fatigue tests. *Materials Science and Engineering: A*, 2021, vol. 802, art. 140679. DOI: 10.1016/j.msea.2020.140679.
28. Savrai R.A., Kolobylin Yu.M., Volkova E.G. Micromechanical characteristics of the surface layer of metastable austenitic steel after frictional treatment. *Physics of Metals and Metallography*, 2021, vol. 122, iss. 8, pp. 800–806. DOI: 10.1134/S0031918X21080123.
29. Vladimirov V.I. *Fizicheskaya priroda razrusheniya materialov* [The physical nature of the destruction of materials]. Moscow, Metallurgiya Publ., 1984. 280 p.
30. Smirnov S.V., Shveikin V.P. *Plastichnost' i deformiruemost' uglerodistykh staley pri obrabotke davleniem* [Ductility and deformability of carbon steels during pressure treatment]. Ekaterinburg, US RAS Publ., 2009. 255 p. ISBN 973-5-7691-2081-7.
31. Kragel'skii I.V., Dobyichin M.N., Kombalov V.S. *Osnovy raschetov na trenie i iznos* [Fundamentals of friction and wear calculations]. Moscow, Mashinostroenie Publ., 1977. 526 p.
32. Korshunov L.G., Shabashov V.A., Chernenko N.L., Pilyugin V.P. The effect of contact stresses on the phase composition, strength and tribological properties of nanocrystal structures formed in steels and alloys upon sliding friction. *Metal Science and Heat Treatment*, 2008, vol. 50, iss. 11–12, pp. 583–592. DOI: 10.1007/s11041-009-9103-2.
33. Jiang W.H., Pinkerton F.E., Atzmon M. Deformation-induced nanocrystallization: A comparison of two amorphous Al-based alloys. *Journal of Materials Research*, 2005, vol. 20, iss. 3, pp. 696–702. DOI: 10.1557/JMR.2005.0090.



34. Mordyuk B.N., Prokopenko G.I. Ultrasonic impact peening for the surface properties management. *Journal of Sound and Vibration*, 2007, vol. 308, pp. 855–866. DOI: 10.1016/j.jsv.2007.03.054.
35. Mordyuk B.N., Prokopenko G.I., Vasylyev M.A., Iefimov M.O. Effect of structure evolution induced by ultrasonic peening on the corrosion behavior of AISI-321 stainless steel. *Materials Science and Engineering: A*, 2007, vol. 458, pp. 253–261. DOI: 10.1016/j.msea.2006.12.049.
36. Rybal'chenko O.V., Dobatkin S.V., Kaputkina L.M., Raab G.I., Krasilnikov N.A. Strength of ultrafine-grained corrosion-resistant steels after severe plastic deformation. *Materials Science and Engineering: A*, 2004, vol. 387–389, pp. 244–248. DOI: 10.1016/j.msea.2004.03.097.
37. Roland T., Reirant D., Lu K., Lu J. Fatigue life improvement through surface nanostructuring of stainless steel by means of surface mechanical attrition treatment. *Scripta Materialia*, 2006, vol. 54, iss. 11, pp. 1949–1954. DOI: 10.1016/j.scriptamat.2006.01.049.
38. Roland T., Reirant D., Lu K., Lu J. Enhanced mechanical behavior of a nanocrystallised stainless steel and its thermal stability. *Materials Science and Engineering: A*, 2007, vol. 445–446, pp. 281–288. DOI: 10.1016/j.msea.2006.09.041.
39. Kuznetsov V.P., Makarov A.V., Psakhie S.G., Savrai R.A., Malygina I.Y., Davydova N.A. Tribological aspects in nanostructuring burnishing of structural steels. *Physical Mesomechanics*, 2014, vol. 17 (4), pp. 250–264. DOI: 10.1134/S102995991404002X.
40. Korshunov L.G. Structure transformations during friction and wear resistance of austenitic steels. *Physics of Metals and Metallography*, 1992, vol. 74, iss. 2, pp. 150–162.
41. Heilmann P., Clark W.A., Rigney D.A. Orientation determination of subsurface cells generated by sliding. *Acta Metallurgica*, 1983, vol. 31, iss. 8, pp. 1293–1305.

Conflicts of Interest

The authors declare no conflict of interest.

© 2022 The Authors. Published by Novosibirsk State Technical University. This is an open access article under the CC BY license (<http://creativecommons.org/licenses/by/4.0/>).